

# EXPERIENCE WITH PSI'S MAIN RING CYCLOTRON LONG RADIAL PROBE

M. Sapinski\*, S. Lindner, R. Martinie, M. Rohrer  
Paul Scherrer Institut, Villigen, Switzerland

## Abstract

A Long Radial Probe is a device used to measure the transverse beam profile in a cyclotron along its radius. The current iteration of the probe was installed in the PSI Main Ring Cyclotron in 2022. After a successful start, the probe encountered issues due to strong coupling with RF fields leaking from the cavities, which resulted in the breakage of the carbon fibers. A series of corrective measures were attempted, but the initial results were inconclusive. This paper discusses the challenges faced and presents the experiments and thermal calculations that provided insights into the RF heating issue.

## INTRODUCTION

A new Long Radial Probe (RRL) was installed in PSI Main Ring Cyclotron in 2022. Its initially successful commissioning is described in [1] (see also references therein). The probe demonstrated its usefulness in measuring beam profiles across the entire beam current range, from single A up to 1.8 mA. However, after a few months of operation, several issues remained, including:

- Thermionic emission was observed and only partially suppressed, as described in [2].
- Activation hot spot has been found on the RRL structure and investigated, as described [3]. As a countermeasure the entire RRL structure has been motorized and is removed from the machine when not in used.
- A frequent generation of interlocks due to proximity of electrostatic injection septum has been observed and this issue is still under investigation.

None of the aforementioned problems have prevent the RRL from obtaining useful data on beam profiles. However, already in August 2022, the wires began to break even at low beam currents. The problem worsened during the remaining months of 2022 and persisted during the operation in 2023. The newly installed wires were damaged solely by RF fields, without the presence of a beam. We focused on investigating this critical issue and those efforts are described here.

## MOVING SUPPORT DESIGN

The three wires used to measure the profile of the beam are attached to two trolleys, upper and lower one, driven by the same motor which moves two transmission belts synchronously. The two trolleys, shown in Fig. 1, can be installed and removed as a complete unit using an auxiliary

device. Only the two electrical plugs, carrying the probe signals, need to be disconnected. Aluminium covers, protecting the cables from the RF fields, are not shown in Fig. 1, but can be partly seen in Fig. 2.

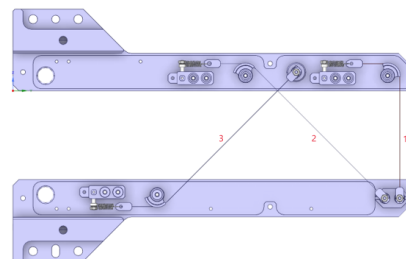


Figure 1: Layout of the RRL trolleys with covers removed.

The wires are made of 33  $\mu\text{m}$  carbon fibers, which are glued to small pads made of beryllium copper (CuBe) alloy, using conductive adhesive as shown in Fig. 3. One pad is directly connected to a metallic pin that transmits the signal to the readout cable. The other pad is attached to a spring to accommodate variations in the movement of the two trolleys. In order to accommodate spring length the wires are bend 45° or 90° using deflection rollers.

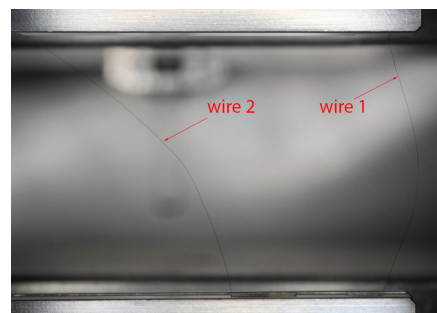


Figure 2: Typical view of damaged RRL wires obtained using Sigma 105 mm macro lens on full frame camera.

The numbering of the wires is from the right to left (see Fig. 1), i.e. the vertical wire is called *wire 1* and the two tilted wires are called *wire 2* and *wire 3*.

## WIRE FAILURE

The glowing of the wire due to high temperatures induced by coupling to the RF field has been described in [1]. However, during the scans without the beam, no thermionic current was observed, indicating that the wire's temperature must have been below approximately 1700 °C - the threshold at which thermionic current should be observable with the LogIV4x4 current acquisition module, which has sensitivity

\* mariusz.sapinski@psi.ch

of about 10 pA. This allows us to estimate that the RF power transferred to the exposed part of the wire is less than 2.5 W.

It has been observed that the wire failures are not caused by the rupture of the wire itself, but rather due to the detachment of the wire from its fixation points. The typical situation after such a failure is shown in Fig. 2, where two out of three wires are visible. Both wires have lost their tension and are likely making electrical contact with the aluminum shield of the trolley, which means that they do not provide a good signal anymore. Further investigation often revealed that the wires were not anymore attached to the pins. Initially, it was concluded that the wire heating caused loosening of the prespring and, combined with vibrations during the movement of the trolleys, this led to wires detaching from the pins.



Figure 3: An image of the CuBe pad with glue and wire obtained using Dino-Lite AM7013MT digital microscope.

As a countermeasure the pins were replaced with screws, and the wires were secured using nuts; however, this did not resolve the issue. The next observation was critical: in multiple cases the wires appeared to be broken at the surface of the glue. Through a series of experiments, it was proven that the mechanism is not actually a breakage of the wires, but a result of the wires slipping out of the glue. That is most likely due to change of glue's properties with temperature.

It is important to note that the wires differ in vulnerability. It has been observed that the wire 1 glows the brightest and is the first to fail. Wires 2 and 3 exhibit similar behaviour, with wire 3 being slightly more prone to failures than wire 2. The reasons for these differences could be:

- Stronger RF coupling to the vertical wire due to RF field configuration and lower resistance of the wire.
- A shorter portion of the wire being protected by the shields.
- Additional tension and vibration caused by the spring location in the bottom trolley for wire 3.

## LAB EXPERIMENTS

A simplified setup containing only one wire was placed in a vacuum bell to investigate the performance of the adhesives. The wire was heated using Joule heating, which produces uniform heating power along the wire, in contrast

to the more localized RF-heating experienced in the machine. Additionally, the heating was also not limited to the duration of a scan (approximately 3 minutes), making the experimental conditions more severe than those in actual operation.

The current and voltage were increased in steps until the observation of the rupture. The total power fed to the system is:  $P = U \cdot I$ . The glowing of the wire was observed already for power of 0.5 W. In almost all cases the failure was due to the wire slipping out of the glue. Results are shown in Fig. 4. The *radiative temperature* is calculated assuming a steady state condition where all the input power is evacuated by radiative cooling:

$$P \cdot U = \epsilon \sigma A_{rad}(T^4 - T_{amb}^4) \quad (1)$$

where  $\epsilon$  is material emissivity (close to 1 in case of graphite),  $\sigma$  is Stefan-Boltzmann constant and ambient temperature  $T_{amb}$  is assumed to be 24 °C. It is an approximate equation which overestimates the temperature, however it was shown in [4] that in the expected temperature range the radiative cooling is a dominant cooling process.

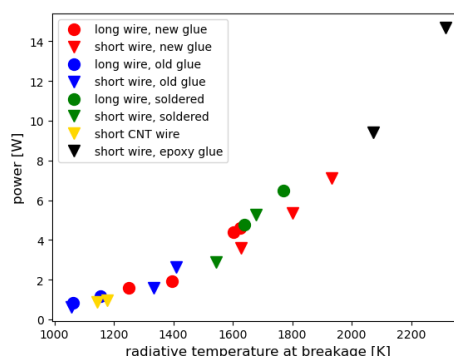


Figure 4: Summary of experimental results.

The performance of the old glue is clearly inferior to that of the new glue or even standard solder. Epoxy glue, which has yet to be tested in the machine, has shown the ability to withstand nearly twice the heating power compared to other materials. However, the results are highly variable across all types of adhesives, suggesting that other factors, not accounted for in this measurement - such as heating duration, the amount of used glue, etc. - play a significant role. These measurement also reveal a weak temperature dependence of electrical resistivity between 20 and 30 m for temperatures up to 2000 K.

## ANSYS SIMULATIONS

Steady-state thermal and thermal-electrical ANSYS simulations have been performed to estimate on one hand the temperature of the metal pads to which the glue is applied and on the other hand the influence of the location of the internal heat generation. For the simulations, only the geometry of wire 1 was considered. It consists of the carbon wire, the CuBe pads at both ends and the aluminum deflection

roller that bends the wire toward the left in Fig. 1. Two heat loads were considered:

- Load 1: uniform heat generation in the volume of the wire located in between the forks. This case is considered similar to the real conditions. It is also the more optimistic case since it assumes that no RF leakage occurs outside of the space between the forks and the heating profile along the wire segment is uniform.
- Load 2: resistive heating between the metal pads. This is the worst case scenario since the heat generation occurs all along the wire. It simulates the lab experiments presented in the previous section.

For each heat load, several simulations were ran while increasing the magnitude of the internal heat generation (load 1) or current (load 2). Temperature dependent material properties were considered and since the carbon wire material properties are unknown, graphite properties were used. The wire emissivity was set to 0.7 and 0.1 for the metal pads. A constant temperature of 22 °C was applied to the inner hole of the deflection roller.

Finally, perfect thermal contacts were assumed and the wire goes through the CuBe pads. No glue nor solder was included in the geometry.

### Load 1 - Heat Generation Between the Trolleys

The temperature distribution along the wire is plotted in Fig. 5. The temperature at the extremities of the wire is independent of the magnitude of the internal heat generation. Since thermal radiation is the main cooling process, the temperature drops significantly outside of the volume where the heat generation is located. It is worth noticing that the temperature at the aluminum deflection roller drops to 23 °C.

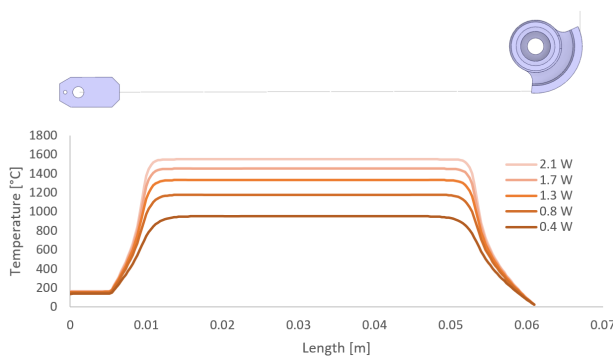


Figure 5: ANSYS simulations load 1: temperature distribution along the wire for various internal heat generations.

### Load 2 - Joule Heating

The electrical boundary conditions consist of 0 V at one end of the wire and a current ranging from 10 to 50 mA at the other end. A constant resistivity of the carbon wire of 20  $\mu\Omega\cdot\text{m}$  was estimated from the current-voltage measurements presented in the previous section.

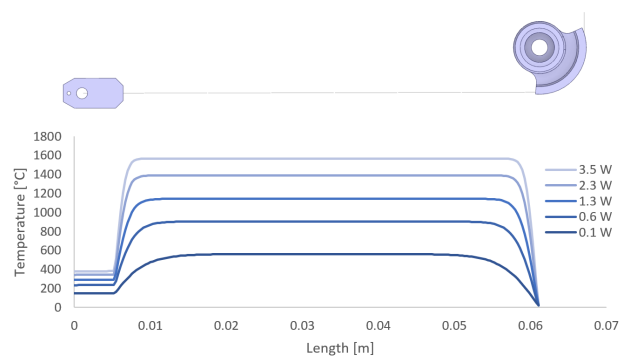


Figure 6: ANSYS simulations load 2: temperature distribution along the wire for various heat generation.

In this situation, shown in Fig. 6, the temperature of the metal pad is strongly related to the temperature of the wire and reaches up to 400 °C at 3.5 W. Even though it is not represented on the figure, the temperature of the other metal pad is similar to the one shown here.

### Conclusion of the ANSYS Simulations

Figure 7 shows the temperature of the metal pads as a function of the wire temperature. It is believed that between the two curves lies the situation that can be found in the main ring cyclotron and it is most likely close to load 2 i.e. that there are RF leakages within the forks. Otherwise, the wire cools down significantly before reaching the metal pads. The simulations show that the use of an adhesive material with higher failure temperature would help.

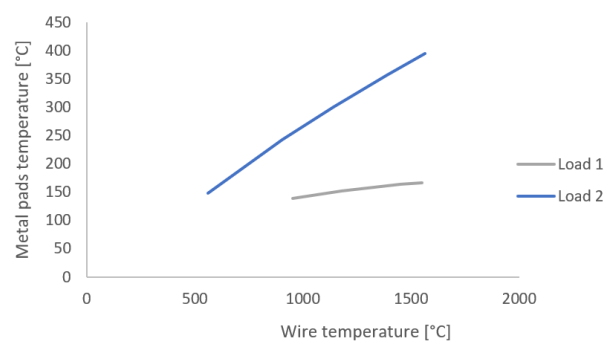


Figure 7: ANSYS Conclusion - Temperature of the metal pads as a function of the wire temperature.

Finally in both simulated loads, the temperature of the wire drops to 22 °C at the deflection roller. This might not reflect totally the reality for two reasons. The thermal contacts might not be perfect and the boundary condition of 22 °C might be too strong and not so representative. It is however sure that the temperature of the wire at this location drops below 1000 °C since it was observed during the experiments that the wire does not glow while in contact with the deflection roller.



## COUNTERMEASURES

The final effective countermeasures are based on a choice of materials with better high-temperature properties (see Table 1) and reduction of RF leak into the trolleys.

### *New Glues and Solders*

Once it was observed that the common mode of wire failure involved the wire slipping out of the glue, alternative methods for securing the wire were explored. Resbond 931C glue was acquired for testing, as it is specified to retain its properties up to the temperatures of about 1300 °C.

The initial tests were promising. Figure 4 shows a superior performance of the wires prepared using the new glue. These wires were installed in the machine and lasted several months, with only wire 1 damaged after several scans. The damage mechanism appeared to be the same as before - slipping out of the glue.

However, Resbond glue changes its properties over time, losing strength several months after the container is first opened. Additionally it is expensive. Therefore tests with standard soft solder (Sn60Pb40, melting point 183 °C) and Castolin Eucectic 157 solder (Sn96Ag4 melting point 221 °C) have been conducted. Currently, the Castolin solder is successfully used to fix the wire, however investigations continue towards higher-temperature solder materials and other conductive glues as wire 1 still breaks after small number of scans. Recently tested epoxy glue shows excellent performance, but it has yet to be proven in the machine.

### *Aluminum Nitride Insulators*

Insulating elements are used to electrically separate wires from the trolleys. Initially, alumina ( $Al_2O_3$ ) was used, but it was later replaced by silica due to its smaller permittivity, which led to reduced capacitance between the wire and the trolley and thus potentially weaker RF-coupling. However, it was later argued that the low thermal conductivity of silica can lead to less effective heat dissipation from the wire. This concern was neither confirmed by the simulations nor by observations. The currently used insulators are made of aluminum nitride (AlN) with thermal conductivity 250 times greater than that of silica, but the final choice of the insulating material must still be evaluated.

### *Ferrites*

Ferrites are often used to dampen undesired RF fields, as discussed, for instance, in recent paper [5]. ANSYS simulations and observations of the wire-glue bond failure inside the trolley covers suggest a significant RF-field leakage into the trolley. To mitigate this effect, small ferrite pads Exxelia Y94 (Y-Gd-Al-Co) with a Curie temperature of 250 °C, were glued on the internal side of trolley covers. A visual inspection of those pads after a month in the machine, see Fig. 8, revealed discoloration, indicating that they were exposed to high temperatures. This confirms the presence of RF-fields inside the trolley.

Table 1: Thermal Conductivity at Room Temperature and Characteristic Damage Temperature (Melting or Loss of Adhesive Properties) of Various Relevant Materials

Material	Thermal conductivity [W/m · K]	Damage temperature [°C]
old glue	unknown	unknown
Resbond glue	5.76	1300
standard solder	50	183
Castolin solder	unknown	221
Carbon fiber	0.6	~ 3000
silica	1.3	-
alumina	30	-
AlN	321	-

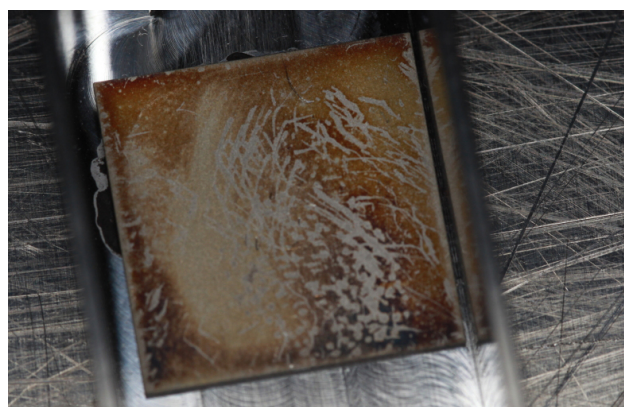


Figure 8: Photo of a ferrite pad taken out of the machine.

Further improvements in the domain of decreasing of the RF intrusion to the trolley is a reduction of openings for the wire passage in the covers.

## CONCLUSIONS

The coupling of the RF fields leaking from the Main Ring Cyclotron cavities to the wires of the Long Radial Probe is a major problem that disrupts the operation of the device. It was found that, at high temperatures, the wires tend to slip out of the conductive glue that connects them to the CuBe pads. Various glues and solders were tested along with installation of ferrites near the most sensitive areas of the device. These measures have significantly improved the durability of the wires, but the optimal solution is still under investigation.

## ACKNOWLEDGEMENTS

Authors want to thanks to Raphael Baldinger, Raffaello Sobbia, Richard Kan and Rudolf Doelling.

## REFERENCES

- [1] M. Sapinski, R. Doelling, and M. Rohrer, "Commissioning of the Renewed Long Radial Probe in PSI Ring Cyclotron", in

*Proc. IBIC'22*, Kraków, Poland, Sep. 2022, pp. 76–79.  
doi : 10.18429/JACoW-IBIC2022-MOP19

- [2] M. Boucard and M. Sapinski, “Dealing with thermionic emission in wire scanners based on secondary electron emission”, in *Proc. IPAC'23*, Venice, Italy, May 2023, pp. 4820–4823.  
doi : 10.18429/JACoW-IPAC2023-THPL150
- [3] M. I. Besana, E. Hohmann, M. Sapinski, J. Snuverink, and D. Werthmüller, “Investigation of Long Radial Probe Activation in the PSI Main Ring Cyclotron”, in *Proc. Cyclotrons'22*, Beijing, China, Dec. 2022, paper WEA005, pp. 163–166.  
doi : 10.18429/JACoW-CYCLOTRONS2022-WEA005
- [4] M. Sapinski, “Model of carbon wire heating in accelerator beam”, CERN, Geneva, Switzerland, Rep. CERN-AB-2008-030, Jul. 2008.
- [5] R. Veness *et al.*, “Overview of Beam Intensity Issues and Mitigations in the CERN-SPS Fast Wire Scanners”, in *Proc. IPAC'24*, Nashville, USA, May 2024, pp. 2248–2251.  
doi : 10.18429/JACoW-IPAC2024-WEPG26